Journal of Structural Geology, Vol. 6, No. 1/2, pp. 19 to 32, 1984
Printed in Great Britain

0191-8141/84 $03.00+0.00
Pergamon Press Ltd.

Calcite fabrics in a natural shear environment, the Helvetic nappes of western Switzerland

DOROTHEE DIETRICH and HONGLIN SONG*

Geologisches Institut, ETH Zentrum, CH-8092 Zürich, Switzerland

(*Accepted in revised form* 28 *June* 1983)

Abstract—The aim of this contribution is to describe and interpret the crystallographic orientations and microstructures of calcite in the Upper Jurassic limestones of the Helvetic nappes between the Mont Blanc and Aar massifs, over a distance along strike of about 180 km.

The *c*-axis preferred orientation pattern, which could be inferred, is regionally very constant. The *c*-axis point maxima are everywhere subperpendicular to the regional strike of the chain. There is an obliquity between the orientation of the macroscopically dominant cleavage and the microscopically visible long axes of individual grains; the *c*-axis maxima in most specimens are parallel to the axis of shortening of the microscopic grain-shape fabric. This fabric geometry indicates either continuous shear deformation, or, alternatively, a two stage deformation history. The obliquity of the grain-shape fabric may be due to the fact that the flattening plane of the individual grains reflects only the last increment of a continuous shear process, or it may represent a later finite deformation, which has led to the formation of a regionally developed second cleavage. There is a systematic relationship between the direction of these late shear movements and the main overthrust direction as given by the finite strain pattern. This suggests that the microfabric of the rocks was acquired during a progressive rotation with time of the main overthrust direction.

The observed pattern of preferred orientation has been correlated by several authors with intracrystalline deformation mechanisms, a combination of slip on *r* and twinning on *e*. However, the *e*-twinning observed in the specimens investigated is younger than the development of the crystallographic fabric.

A new method for stress determination from *e*-twinning is proposed.

INTRODUCTION

DATA on the regional distribution of crystallographic preferred orientations in a deformed geological body are important in structural analysis, because they can reveal information on its deformation history. We have chosen to investigate the calcite fabrics of the Helvetic nappes of western Switzerland, because for them there is some independent information on their deformational state and history (Ayrton 1980, Badoux 1963, 1965, 1970, Collet 1927, Casey *et al.* 1983, Dietrich *et al.* 1983, Durney 1971, Durney & Ramsay 1973, Gray and Durney 1979, Heim 1921, Masson *et al.* in Trümpy 1980, Ramsay 1981, 1982, Ramsay *et al.* 1983, Schmid *et al.* 1981). It is therefore possible to integrate the pattern of crystallographic preferred orientations obtained into a regional tectonic model.

Figure 1 shows a tectonic sketch map of the region studied. The structural pattern of the Helvetic chain is characterized by axial culminations over the Aiguilles Rouges–Mont Blanc and Aar massifs, and by an axial depression, the Wildstrubel depression, between them. The décollement levels which delimit the individual Helvetic nappes climb from the lower levels of the crust beneath the internal Pennine zone upwards towards the external Helvetic zone, and pass through layers of the overlying Mesozoic and Tertiary sediments to give rise first to the most internal of the Helvetic nappes, the Wildhorn nappe. Underlying branch thrusts give rise to the intermediate Diablerets–Gellihorn nappe and, to the most external, the Morcles–Doldenhorn nappe. Each nappe has its own finite strain pattern, as is apparent from the finite strain, $1 + e_1$, trajectories in Fig. 1. The observation that the thrust contacts of the individual nappes show folding of increasing amplitude from the structurally lowest Morcles nappe through the Diablerets and Wildhorn nappes to the basal thrust of the highest Ultrahelvetic nappes is clear geometrical evidence for sequential thrusting from the internal towards the external zones. Figure 2 shows the basal thrust of the Morcles nappe and the deformed thrust contact of the overlying Diablerets nappe. We assume the nappes to have been formed in a shear regime between the overriding Pennine chain and the underlying European foreland (Ramsay *et al.* 1983). The principal effects of deformation in outcrop scale, as the formation of cleavage and lineations, and the production of the rock microstructure and texture appear to be predominantly the result of simple shear.

In shear deformation the finite strain axes and the incremental strain and stress axes are not parallel. In naturally deformed rocks, indicators of the incremental strain/stress axes are often difficult to detect. In the Helvetic nappes there exists a well-preserved syntectonic microfabric, which has been found to be generally oblique to the macroscopic fabric, and which can be interpreted as being the result of a lack of coincidence between the incremental and the finite strain axes during deformation. Schmid *et al.* (1981) have observed an obliquity between the grain-shape fabric and the macroscopic cleavage in limestones from two localities of the Morcles nappe, whereby the *c*-axis maximum was sub-

* Permanent address: Wuhan Geological Institute, Wuhan, Peoples Republic of China.

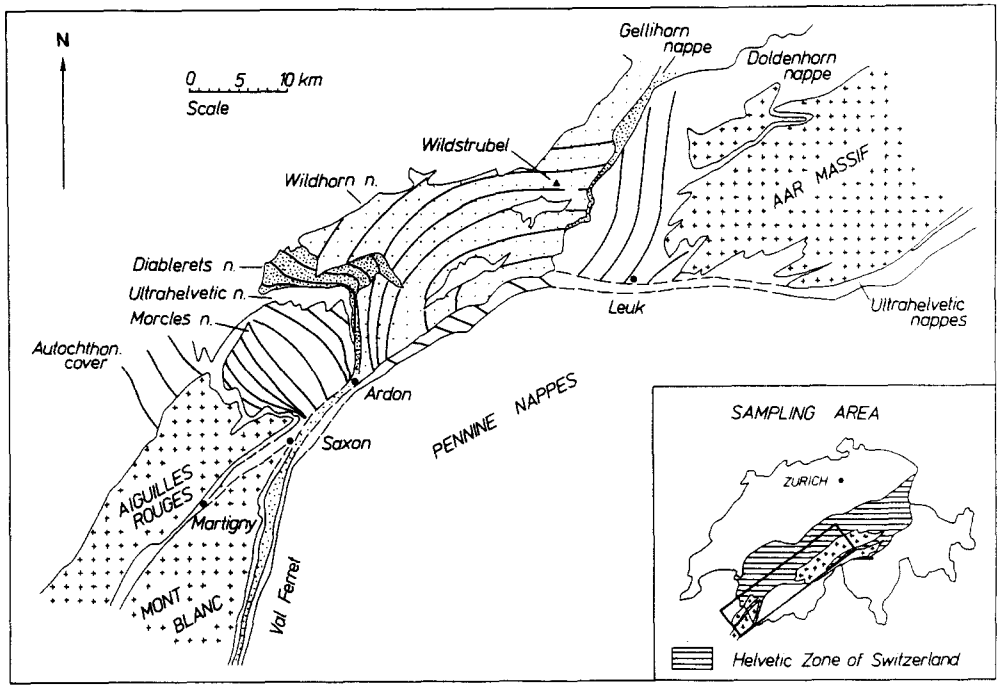

Fig. 1. Tectonic sketch map of the Helvetic nappes of western Switzerland. The finite strain $(1 + e_1)$ trajectories are indicated.

perpendicular to the axis of elongation of the grains. They interpreted this obliquity as the result of a rotational strain path. We have found that this obliquity is a characteristic regional feature of the extremely fine-grained limestones in the Helvetic root zone between the Mont Blanc and the Aar massif, and it has been possible to use the degree of obliquity between the two planar fabrics to quantify the shear movements by which they originated.

THE ROCK MATERIAL INVESTIGATED

The Upper Jurassic limestones (Malm) of the Helvetic nappes are very fine grained, homogeneous and pure. They represent a principal competent layer in all the three nappes. The degree of deformation recorded in these limestones increases in each individual nappe from the northwest towards the southeast. Finite strain values calculated from pressure shadow fibres indicate a maximum extension of $1 < 1 + e_1 < 2$ in the northwestern, frontal part of the nappes, and an increase to $1 + e_1 > 10$ in the southeastern part, or root zone, of the nappes. All three nappes show similar high strain values in the root zone, but the strains in the uppermost Wildhorn nappe decrease faster towards the northwest than the strains in the underlying Diablerets and Morcles nappes.

Fig. 2. A profile across the Morcles nappe, constructed perpendicular to the mean fold axis plunge.

We have concentrated our analysis mainly on the Upper Jurassic limestones from the root zone, and the specimens examined were collected from a distance along-strike of about 180 km. These limestones are characterized by a well-developed slaty cleavage defined by concentrations of clay minerals in millimetric to submillimetric layers. Pressure solution seams are subparallel to the cleavage planes. We assume that the cleavage is parallel to the *XY* plane of the finite strain ellipsoid. This assumption holds to a first approximation, as shown by comparison with finite strain markers such as deformed fossils (echinoids, belemnites, ammonites, gastropods), deformed pebbles, ooids and syntectonic fibres in veins and pressure shadows (Badoux 1963, 1965, 1970, Casey *et al.* 1983, Durney 1971, Durney & Ramsay 1973, and data by D. Dietrich, J. Ramsay and A. Siddans). Bedding is at a very small angle to the cleavage and is not always easy to detect. On the cleavage planes there are two lineations. The first is dominant and represents a stretching lineation, L_1, subparallel to the finite strain trajectories shown in Fig. 1. The second is a more weakly developed lineation, L_2, which has been interpreted as an intersection lineation between the pervasive cleavage and a later second phase cleavage (Durney 1971, Masson *et al.* in Trümpy 1980). The macroscopically dominant cleavage is axial planar to the main first-phase folds, while the second-phase cleavage is axial planar to later minor folds. Figures 3 and 11 illustrate the macroscopic fabric elements of the specimens studied, and Fig. 4 gives the specimen localities. No specimens were collected close to late minor folds, and in no sample has a macroscopically visible second cleavage been observed.

The strike of the Helvetic root zone is not parallel to the metamorphic isograds. Table 1 gives the average calcite grain size of some of the specimens studied. An increase in metamorphism from the central part of the region towards both west and east has given rise to an increase in grain size and to a change in the mineralogical composition of the limestones. Clay minerals, which are present in 1–3 μm thick seams in the central part are replaced by white micas in the west (specimens 540 and 544, Fig. 4) as well as in the east (specimens 481, 488 and 490, Figs. 4 and 5). The crystallographic preferred orientation of calcite was determined by X-ray texture goniometry in the fine-grained, mineralogically homogeneous specimens, while in the coarse-grained specimens the determinations were made using a U-stage.

X-RAY TEXTURE ANALYSIS

The orientations of the [11$\bar{2}$0] planes, or *a*-planes, of calcite were determined with the computer-controlled texture goniometer of the Geologisches Institut, ETH Zürich (combined reflection- and transmission scan method, CoKα-radiation, counting time 50 sec for each 5° step in azimuth and tilt and 100 sec on two background positions after every increment tilt, see Casey *et al.* 1978, Schmid *et al.* 1981, Siddans 1976).

The specimens were cut parallel to the stretching lineation L_1, and perpendicular to the cleavage. The pole figures obtained were subsequently rotated so that north on the pole figures corresponds to geographical north. Figure 3 shows the rotated pole figures obtained; the contours represent multiples of a uniform distribution.

There exists in all specimens a good preferred orientation of the calcite *a*-planes. The pole figures of Fig. 3 show great circle patterns, with a weak tendency for a submaximum to develop in the great circles. This *a*-

Table 1. Grain sizes of selected specimens

Specimen number	Locality	Formation	Grain size short axis/long axis mm	Grain ratio short axis/ long axis	*E*-twinning
400	Ardon	Malm limest.	0.009/0.046 average	1/5	rare
			0.16/0.24 bigger grains	1/1.5	present
430	Wildhorn n.	Malm limest.	0.002/0.003 average	1/1.5	no
			0.08/0.14 bigger grains	1/1.7	no
447	Leuk	Malm limest.	0.018/0.051 average	1/2.8	present
			0.105/0.24 bigger grains	1/2.3	present
468	Fernigen	Malm limest.	0.0046/0.0184 average	1/4	no
			0.064/0.16 bigger grains	1/2.5	no
473	Fernigen	Malm limest.	0.004/0.02 average	1/5	no
			0.03/0.09 bigger grains	1/3	no
481	Andermatt	Malm marble	0.192/0.6	1/3	present
488	Furka Pass	Lias limest.	0.223/0.546	1/2.5	present
490	Furka Pass	Malm limest.	0.104/0.492	1/4.7	present
540	Courmayeur	Malm limest.	0.035/0.103 average	1/3	rare
			0.104/0.58 bigger grains	1/5.6	rare
542	NE Chamonix	Malm limest.	0.012/0.051	1/4.3	rare
544	Val Ferret	Malm limest.	0.039/0.154 average	1/4	rare
			0.075/0.348 bigger grains	1/4.7	rare
549	Val Ferret	Malm limest.	0.015/0.075	1/5	very rare
551	Martigny	Malm limest.	0.062/0.158 average	1/2.6	abundant
			2.029/2.32 bigger grains	1/1.2	abundant
553	Saxon	Malm limest.	0.007/0.023 average	1/3.3	no
			0.046/0.092 bigger grains	1/2	no

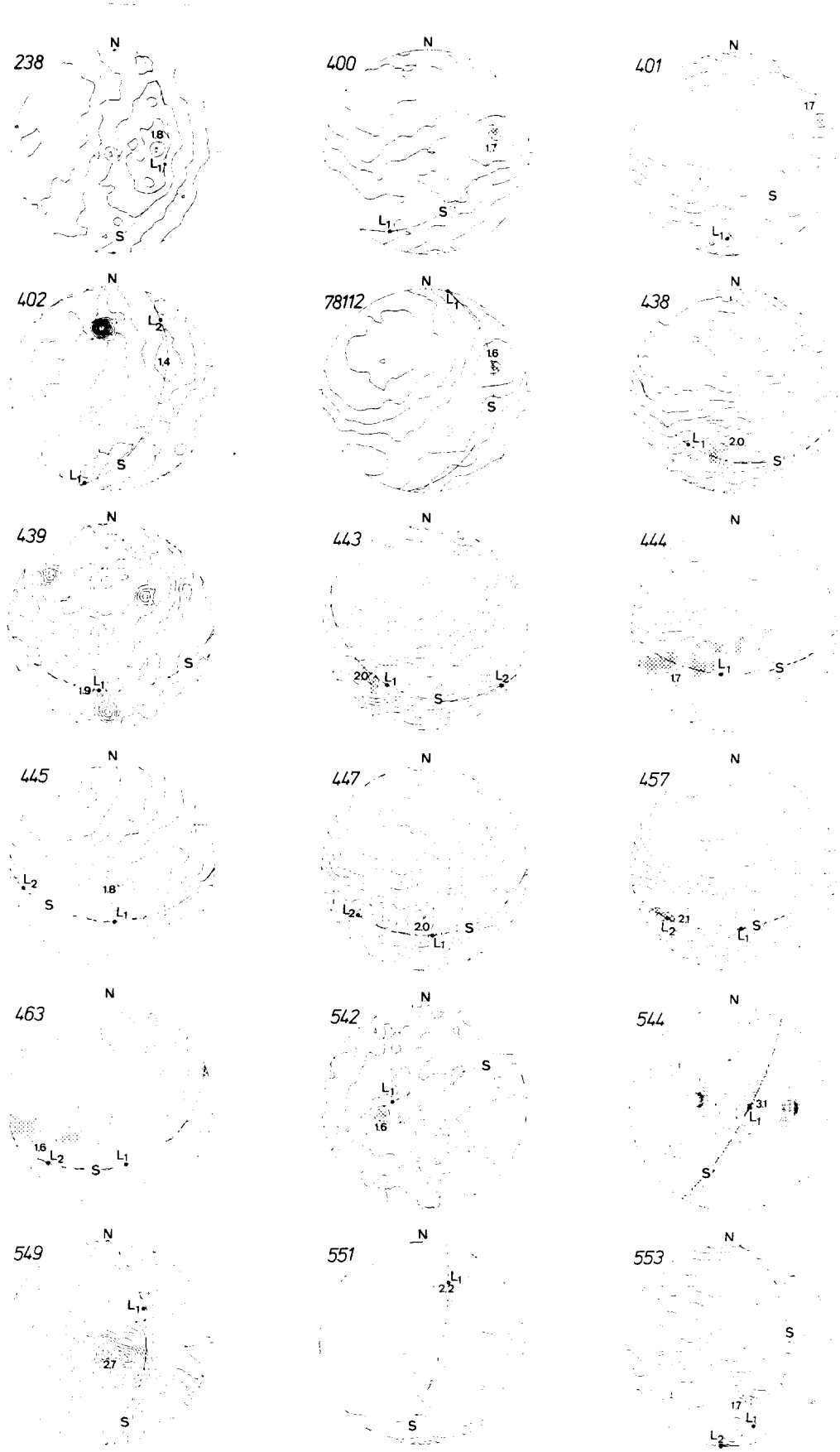

Fig. 3. Calcite *a*-pole figures, measured by X-ray texture goniometry. Specimen localities are given in Fig. 4. Lower-hemisphere equal-area projection. Contour intervals 0.2 times uniform, maximum values are indicated. *S*: plane of macroscopic cleavage. L_1 and L_2: macroscopic lineations. Specimen 78112 measured by S. Schmid and rotated by us to geographical coordinates.

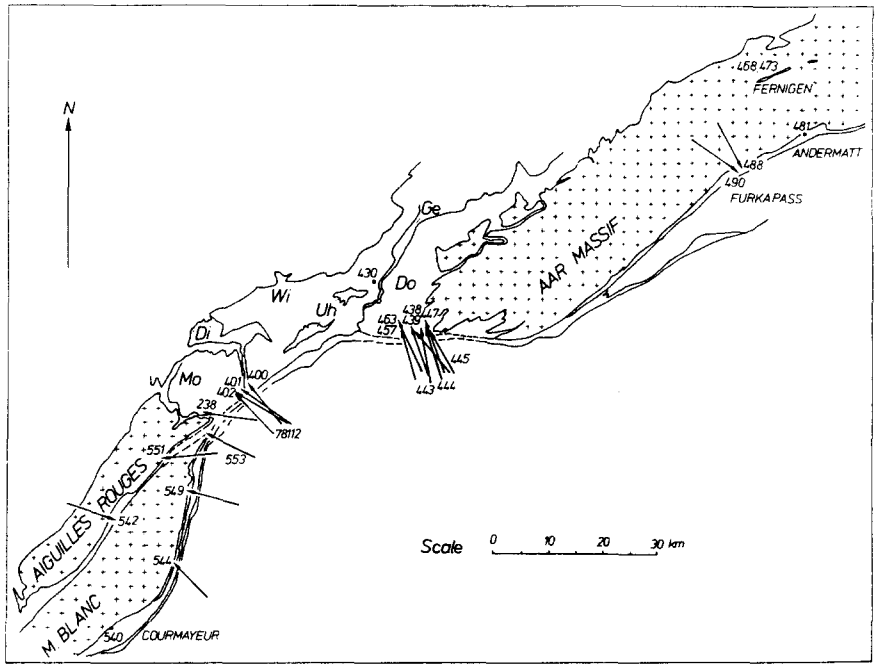

Fig. 4. Calcite *c*-axis pattern, inferred from calcite *a*-pole figures of Fig. 3 and from optical *c*-axis measurements of Fig. 11. Arrowheads indicate specimen localities and point down-dip. Mo, Morcles nappe; Di, Diablerets nappe; Wi, Wildhorn nappe; Uh, Ultrahelvetic nappes; Ge, Gellihorn nappe; Do, Doldenhorn nappe.

maximum is especially strongly developed in three specimens from the western part of the region, 542, 544 and 551, and tends to obliterate the great circle pattern. Specimens 402, 439 and 544 show additional maxima outside of the great circle which are due only to the statistical effect of individual bigger crystals present in these specimens. The orientation of the *a*-great circles is regionally very constant. They do not coincide with the macroscopic cleavage plane, labelled 'S' in Fig. 3. There is no close correspondence between the *a*-maxima and the macroscopic lineations L_1 and L_2.

Since the poles to the calcite *a*-planes are perpendicular to the *c*-axis, the position of the *c*-axis point maximum can be inferred: it coincides with the *a*-minimum in the pole figures of Fig. 3. This has been confirmed by the measured *c*-pole figures of Schmid *et al.* (1981) and of this work (Fig. 6). The regional variation of the inferred *c*-axis point maxima is shown in Fig. 4. The azimuths of the *c*-axis maxima are everywhere at a high angle to the strike of the chain and change direction from east to west. It follows from Fig. 3 that the *c*-axis maxima are oblique to the macroscopic cleavage.

No preferred orientation of the *a*-planes has been found for specimen 430 from the Wildhorn nappe, taken from a locality about 10 km northwest of the root zone and of a lower finite strain state ($1 + e_1 = 2.3$ measured from pressure shadow fibres close to the specimen locality, and in the same rock type). A preferred orientation of the *a*-planes is also absent in the four specimens from the Fernigen syncline, a syncline of Helvetic sediments within the Aar massif (locality indicated in Fig. 4), where the finite strain as determined from pressure shadows, amounts to $1 + e_1 > 10$.

MICROSTRUCTURE

Some aspects of the microstructural pattern related to this type of texture have been already discussed by Schmid *et al.* (1981) and by Schmid (1982). In this section we summarize the main features, and add some further observations.

Figure 5 shows three photomicrographs of perpendicular sections of specimen 447 (from the Doldenhorn nappe, locality Hohe Brücke near Leuk, Figs. 1 and 4). The orientation of the micrographs relative to the specimen is given on the sketch in Fig. 5. Surface C of the cube represents the macroscopic cleavage plane, surface A is perpendicular to the cleavage and to L_2, and surface B is perpendicular to the cleavage and parallel to L_2. The most striking feature of micrograph A is, that the grains define a plane of mean elongation which is inclined at about 20° to the macroscopic cleavage. Such an obliquity between the macroscopic and microscopic fabric is characteristic of all the specimens showing a preferred orientation of *a*-planes. A comparison of this obliquity in thin sections and in pole figures of identical orientation shows that the planes of mean grain elongation correspond with the *a*-great circles, that is the inferred *c*-axis maxima are perpendicular to the planar grain-shape fabric. In specimen 447 the highest degree of obliquity, 19°, is observed in a section perpendicular to L_2. The angle between the *c*-axis maximum and L_2 is about 90° in four of the seven pole figures of Fig. 3, in which a second lineation was present. For specimens 443, 445 and 553 this angle is respectively 112, 70 and 108°. There is therefore no direct relationship between L_2 and the crystallographic fabric. The stretching lineation L_1 and

the crystallographic fabric can not be related by a simple kinematic model. It can be concluded that both macroscopic lineations are older than the development of the crystallographic fabric and the grain-shape fabric. It should be noted that the bigger grains often show a smaller degree of obliquity relative to the macroscopic cleavage than do the smaller grains.

Micrograph B shows that the grains are flattened. The aspect ratios of the grains do not correspond with the amount of finite strain in the nearby rock. Pressure shadows in the same rock type from a locality about 300 m away from that of specimen 447 give values for the finite strain axes $X:Y:Z$ of 30:8:1. The ratio $X:Z$ of the longest grain in micrograph A is only 5:1. The grain boundaries are serrated, particularly evident in micrograph A, suggesting that grain boundary migration might be the reason for the lack of coincidence between the finite strain state of the rock and the aspect ratios of the grains. Serrated grain boundaries are generally observed in those areas of the specimens where bigger intraclasts are present. There is everywhere a tendency for the grains to revert to equidimensional shapes with equilibrated grain boundaries, and areas with isometric grains and fairly straight grain boundaries can be found in most specimens. Schmid *et al.* (1981) give a good example with their fig. 4(c).

Micrograph C shows strikingly that there are no pronounced lineations visible in thin sections cut parallel to the cleavage plane, notwithstanding that both lineations are well developed in this hand-specimen. The directions of the two lineations are indicated on the micrograph.

Deformation twins are abundant in specimen 447, and can be observed in varying amounts in the other specimens investigated; examples are given in Table 1.

A different microstructure has been found in those specimens which show no preferred orientation of the calcite *a*-planes. Specimen 430 from the external, less deformed part of the Wildhorn nappe shows a mosaic of extremely small grains ($< 5\ \mu$ m), which do not show any grain-shape orientation and are untwinned. The bigger intraclasts present are twinned and elongated subparallel to the pressure solution seams which define the macroscopic cleavage planes in the thin section. The specimens from the Fernigen syncline have a similar small grain size. The matrix grains are also untwinned but are clearly elongated parallel to the macroscopic cleavage plane (Table 1). No difference in microstructure could be detected in the specimens from the lower or upper limb of the syncline; the microscopic and the macroscopic fabrics are here parallel.

COMPARISON WITH THE RESULTS OF EXPERIMENTS AND DISCUSSION

In the limestones of the Helvetic root zone only one type of preferred orientation pattern was found: a single *c*-axis point maximum. The maximum is oblique to the macroscopic rock cleavage and perpendicular to the planar grain-shape fabric. Before attempting to interpret this fabric geometry some pertinent results of experimental deformation of calcite aggregates will be reviewed.

(1) Coaxially deformed calcite rocks develop a preferred orientation of the poles to the $[01\bar{1}2]$ planes, or *e*-planes, parallel to the compression direction, under experimental conditions of low T and high stress, where *e*-twinning dominates (Handin & Griggs 1951, Turner & Chi'h 1951, Turner *et al.* 1956, Wenk *et al.* 1973, Kern 1977, Rutter & Rusbridge 1977, Casey *et al.* 1978). In calcite the angle between the poles to the *e*-planes and the *c*-axis is only 26°. We can assume therefore that the fairly broad *a*-minimum or *c*-maximum of the Helvetic specimens overlaps with the single maximum of the poles to the *e*-planes (Figs. 6d & e and 11d & e) and the *c*- and *e*-pole figures of Schmid *et al.* 1981).

Intracrystalline deformation, a combination of slip on *r* $[10\bar{1}1]$ and twinning on *e*, is held responsible for the development of this preferred orientation pattern (Wenk *et al.* 1973, Casey *et al.* 1978). Because no preferred orientation has been found in the Fernigen specimens, it is suggested that an intercrystalline deformation mechanism such as grain-boundary sliding is responsible for the random texture patterns obtained from this locality.

(2) Calcite fabrics of experimental shear zones have been studied by Rutter & Rusbridge (1977), Friedman & Higgs (1981) and Kern & Wenk (1982). Rutter & Rusbridge (1977) approximated shearing by a two-stage deformation: a first deformation of 30% coaxial shortening resulted in a *c*-axis preferred orientation parallel to the compression direction, and in a planar grain-shape fabric perpendicular to the compression direction. They recut the specimens obliquely to the grain-shape fabric and on further deformation they calculated that again at $> 30\%$ shortening the *c*-axis maximum would coincide with the new compression direction. The grain-shape fabric of their specimens rotated more slowly than did the *c*-axis maximum: at 40% shortening there would still be an angle of 25° between the poles to the grain long axes and the compression direction. They concluded that . . . "whereas grain shape orientation reflected finite strain, crystallographic preferred orientation responds rapidly to variations in the orientation of either stress or incremental strain" (Rutter & Rusbridge 1977, p.83).

Friedmann & Higgs (1981) deformed a cylindrical rock specimen with crushed calcite along a precut surface oriented at 35° to the compression axis, and achieved simple shear deformation of the calcite gouge. In their lower T (400–650°) experiments the *c*-axes of the starting material, which showed only a weak preferred orientation, developed a single point maximum perpendicular to a planar grain-shape fabric. Friedmann & Higgs' interpretation of these particular experiments is that *c*-axes and poles to *e*-lamellae ". . . geometrically track the axis of shortening defined statistically from the short axes of the porphyroclasts, i.e., the normal to the foliation produced by the elongated porphyroclasts" (Friedman & Higgs 1981, p. 23).

Kern & Wenk (1982) produced simple shear deforma-

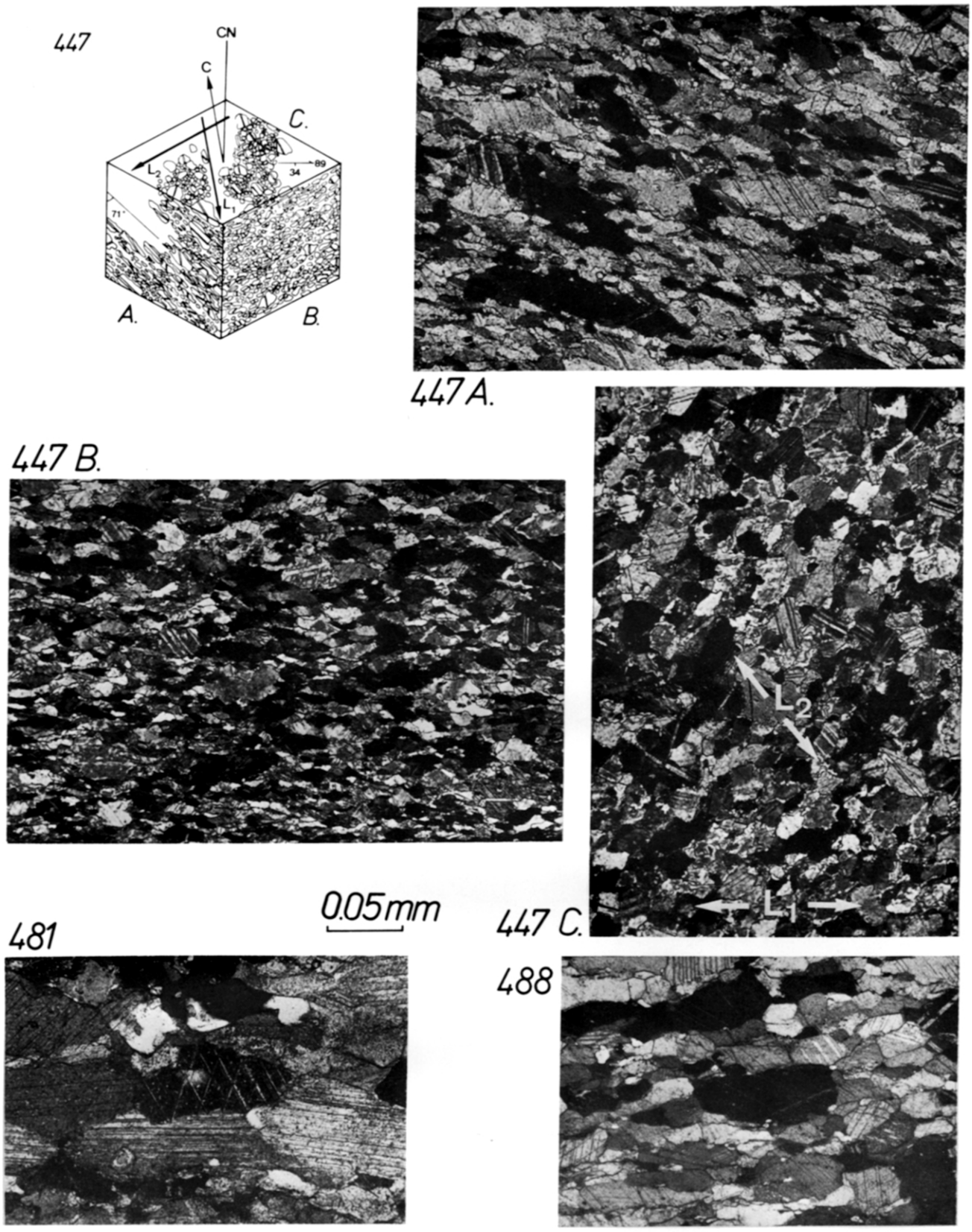

Fig. 5. Photomicrographs of specimen 447, Leuk, Doldenhorn nappe, and of specimens 481, Andermatt, and 488, Furka Pass. The orientation of the three micrographs of specimen 447 is given in the sketch. Specimens 481 and 488 are cut parallel to L_1 and perpendicular to the cleavage. The scale is identical for all the micrographs.

tion in a limestone specimen with a triaxial pressure apparatus at 1 kbar and 400°. They produced a grain-shape fabric which recorded the applied finite strain, and obtained pole figures with three *c*-axis maxima.

None of these experiments can be compared directly with the deformation of the Helvetic limestones. Rutter & Rusbridge (1977) superimposed two flattening deformations, that is they produced a kinematic process which is essentially different from simple shear. Friedman & Higgs' (1981) calcite gouge involves the problem of passive grain rotation, and no quantitative texture determination of all the grains in the shear zone was possible; only the crystallographic orientation of the porphyroblasts could be measured. Kern & Wenk's (1982) pole figures differ from the single maximum pole figures of the Helvetic limestones and suggest that their specimens were deformed by a mechanism different from that of the Helvetic limestones.

But, to the contrary, certain aspects of the experimental results coincide with the observed deformation in the Helvetic rocks and therefore inspire us to an interpretation. Rutter & Rusbridge's (1977) conclusion regarding the obliquity between the crystallographic fabric and the finite strain axes would suggest that the directions of the Helvetic *c*-axis maxima coincide with the directions of σ_1 during the last strain increments, that is a noncoincidence of the incremental strain/stress axes with the finite strain axes in a continuous shear deformation. This interpretation has been envisaged by Schmid *et al.* (1981).

Alternatively one could suggest that the grain-shape fabric and the crystallographic fabric reflect a finite deformation event which is later than the formation of the macroscopic cleavage. The grain-shape fabric would therefore correspond to a second-phase cleavage, slightly more steeply inclined than the macroscopic cleavage. The grain axial ratio would be correlatable with the strain of this later deformation event; the effects of the earlier deformation would be completely overprinted by the new grain-shape and crystallographic fabric.

We favour the second interpretation. This is supported by the following arguments.

(1) The grain-shape and the crystallographic fabric of the specimens investigated are parallel, in correspondance with Friedman & Higgs' (1981) result.

(2) Small-scale folds, which fold the main cleavage, can be found all along the Helvetic root zone. It was observed that in two of such second-phase folds the microscopic grain-shape fabric is parallel to their macroscopically visible axial-plane cleavage.

If this interpretation is correct, and if the fabric did arise through simple shear only, the amount of shear strain responsible for the grain-shape fabric can be calculated (Ramsay 1967, equation 3-67). If the amount of shear strain is known, the position of the shear planes related to the generation of the second-phase cleavage can be determined (Ramsay 1967, equa. 3-70). It has been found for the specimens investigated, that the calculated angle between the grain long axis and the shear plane varies between 20 and 35°, that is it corresponds approximately with the measured angle between the crystallographic fabric and the macroscopic cleavage. Therefore it could be concluded, that cleavage-parallel late shear movements are responsible for the generation of the second-phase cleavage.

It should be mentioned that the grain axial ratios given in Table 1 do not indicate the principal strains of the second phase cleavage, because they were measured in thin sections parallel to L_1 and perpendicular to the macroscopic cleavage, that is in a principal plane of the first phase of deformation, and not of the second phase. From a knowledge of the strain on a single plane and from the given orientation of the principal axes of the ellipsoid the principal strains can be calculated (Ramsay 1967, pp. 148–149). The measured *a*-girdles have been assumed to represent the finite *XY* plane of the second phase cleavage; the *X* direction would be represented by the intersection of the *XY* plane with the plane containing the normal to the macroscopic cleavage and the normal to the *a*-girdle. It was however not found possible to obtain meaningful solutions here as the method applied requires a consistency of data beyond that obtainable from these types of measurements.

Finally it is interesting to note that this second-phase cleavage is not visible macroscopically in the specimens chosen for this study.

OPTICAL ANALYSIS OF CALCITE FABRICS

Those specimens which were unsuitable for texture goniometry because of their grain size and their mineralogical composition have been measured by U-stage methods (Figs. 5 and 11). In order to compare the results of the two methods, we have applied them both to specimen 447. Figure 6 (c) shows the *a*-minimum or *c*-maximum obtained by texture goniometry, and Fig. 6 (d) shows the optically determined *c*-axis preferred orientation for the same specimen. The two pole figures are very similar, notwithstanding that texture goniometry includes the measurements of the twinned volume, that is parts of grains with a *c*-axis rotated by 52.5° relative to the *c*-axis of the host. The optical analysis does not include the *c*-axes of the twinned volume. Evidently, twinning is not intense enough to change the statistical *c*-axis orientation. In fact, the spacing index of the *e*-lamellae is rather low, about 20–60 in the largest grains (Fig. 5).

The *c*-axis preferred orientation found for specimens 488 and 490 from the Helvetic root zone at Furka Pass correlates well with the pattern determined from the specimens measured by texture goniometry; that is the maximum is subperpendicular to the strike of the chain (Fig. 4). Figure 11 (d) indicates that the *c*-axis maxima of both specimens are oblique to the macroscopic cleavage. Specimen 481 from Andermatt is special in that it is the only Helvetic specimen which has not given a *c*-axis point maximum, showing instead a tendency to a girdle distribution (Fig. 11d). The grain-shape fabric is parallel

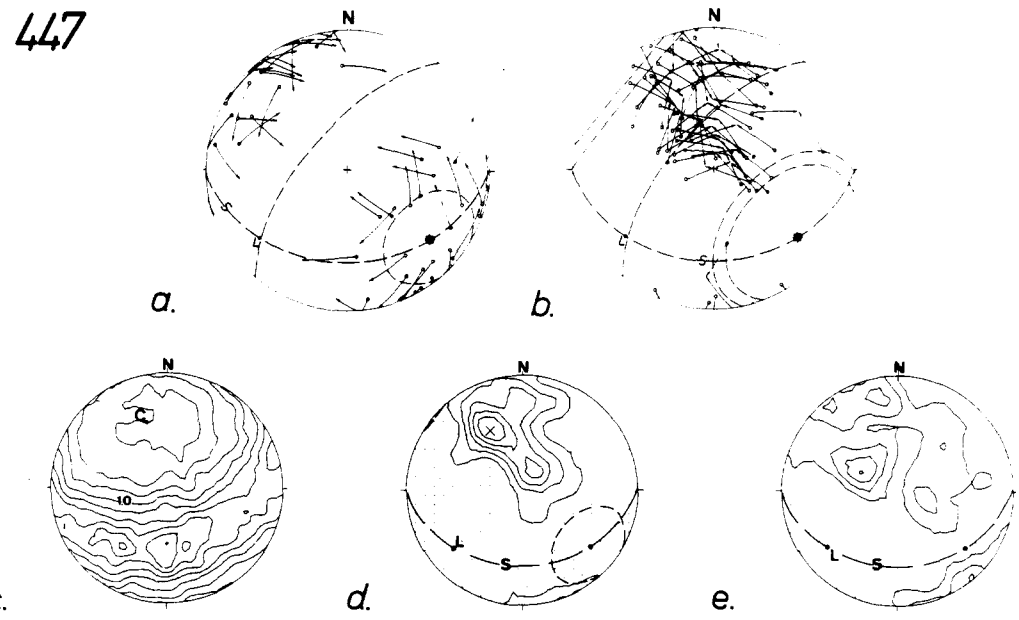

Fig. 6. Specimen 447, Leuk, Doldenhorn nappe. Results of U-stage measurements and comparison with the results of texture goniometry. Lower-hemisphere equal-area projection. *S*, plane of macroscopic cleavage; *L*, macroscopic intersection lineation (L_2). (a) Pole figure for *e* and *c* of calcite grains with one *e*-twin set developed. Open circles-poles to *e*-twin planes. Arrows show the movement direction for *e*-twinning from *e*-poles to *c*-axes. Centre of small circle: σ_1 for *e*-twinning (for method of stress determination see Appendix). (b) Pole figure for *e* and *c* of calcite grains with two or three *e*-twin sets developed. (c) Pole figure for calcite *a*-planes, measured by X-ray texture goniometry. 'C' indicates the inferred *c*-maximum. Contour intervals 0.2 times uniform. (d) Pole figure for calcite *c*-axes from host grains. 96 data, contours at 1, 2, 3, 4, 5 points per 1% area. (e) Pole figure for calcite *e*- twin planes. 156 data, contours at 1, 2, 3, 4 points per 0.6% area.

to the macroscopic cleavage for all three specimens (Fig. 5).

It has been discussed previously why we assume that the *c*-axis maximum is parallel to the compression direction responsible for the grain-shape and the crystallographic fabric of the specimens investigated. For comparison we have constructed the compression direction which can be inferred from *e*-twinning. The optically obtained *e*-pole figures for specimen 447 are given in Fig. 6 (e), and for specimens 481, 488 and 490 in Fig. 11 (e). The method for the determination of σ_1 from *e*-twinning described by Turner & Weiss (1963, pp. 242–243) gave unclear results. Figure 11 (c) shows three pole figures for σ_1 determined following Turner & Weiss (1963), but only in the case of specimen 488 could a clear maximum be obtained; specimen 481 shows three maxima, and specimen 490 shows a girdle. We have developed therefore a new graphical method for the determination of the compression direction from *e*-twinning (see Appendix). Figures 6 (a) and (b) show the result of our method applied to specimen 447. It appears immediately that the compression direction inferred from *e*-twinning differs from the *c*-axis maximum (Figs. 6c & d). A similar lack of coincidence has been found in specimens 481 and 490 (Figs. 11a and b). In specimen 488 the two directions also do not correspond, but Turner & Weiss' (1963) method and our's produced similar results.

It can be deduced from these observations, that the *e*-twinning visible in the Helvetic specimens is later than the development of the *c*-axis preferred orientation. The compression direction inferred from *e*-twinning is subparallel to the macroscopic cleavage, with the exception of specimen 481 from Andermatt. In specimen 447, σ_1 from *e*-twinning is perpendicular to the second lineation, indicated by '*L*' in Fig. 6. This relationship suggests that the macroscopic cleavage/grain-shape fabric intersection lineation keeps its significance as a *b*-axis, using simple shear coordinates, throughout the deformation history.

CONCLUSIONS

The pattern of the *c*-axis preferred orientations determined at several localities along the root zone of the Helvetic nappes is regionally very constant: the *c*-axis maxima are subperpendicular to the strike of the chain, and oblique to the macroscopic cleavage. The *c*-axis maxima are parallel to the short axes of the grains, except for the two specimens from the Furka Pass. The crystallographic fabric is therefore related to the compression axis responsible for the grain-shape fabric. The macroscopic cleavage is parallel to the *XY* plane of the finite strain ellipsoid, as established from finite strain markers. The noncoincidence of the crystallographic and grain-shape fabric with the finite strain fabric indicates either continuous rotational deformation, or, alternatively, a two-stage deformation process. These are two possible interpretations which have distinct consequences on the geological history that is inferred.

As a first model we assumed progressive simple shear deformation, where grain shape and texture relate only to the last strain increments of a continuous deformation process. It is a well-known feature of shear zone geometry that the angle between the shear zone boundary planes and the infinitesimal strain and stress axes is

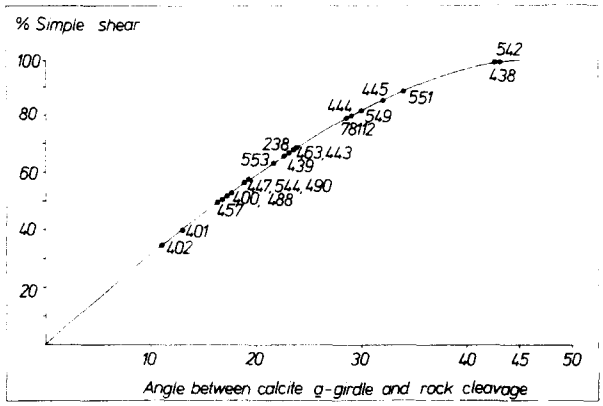

Fig. 7. The angles between the calcite *a*-girdles and the macroscopic cleavage, expressed in percentages of simple shear.

45° (Chapple 1968, Ramsay 1980). The bedding planes represent the principal planes of anisotropy in the Helvetic sequence, and in the root zone of the Helvetic nappes bedding and macroscopic cleavage are subparallel. In outcrop scale there are indications for bedding-parallel shearing (Dietrich *et al.* 1983). Figure 7 shows an attempt at quantifying the shear movements related to the grain-shape and crystallographic fabric. The angles between the *a*-girdles and the macroscopic cleavage planes, that is the angles between the incremental and finite flattening planes, are expressed in percentages of simple shear. 100% simple shear corresponds to the theoretically required angle of 45° between the two flattening planes. The angles measured from the specimens investigated give between 30 and 100% simple shear, indicating the existence of an important component of pure shear and/or flattening deformation. It is however difficult to understand why there is no regionally significant trend in the variation of the percentage simple shear shown in Fig. 7.

Pfiffner & Ramsay (1982, fig. 4) proposed a graphical representation for a steady state rotational deformation, superimposing increments of plane distortion with incremental rotations, and plotting the angles between the principal finite strain axis and the principal incremental strain axis against principal finite strain, $1 + e_1$. The orientation of the flattening plane rapidly approaches an asymptotic value which depends on the ratio of simple shear to pure shear. Figure 8 shows an application of this graph to specimens 78112 and 402, both from the normal limb of the Morcles nappe at Ardon. The assumptions are plane strain deformation and that the incremental principal strain axes are of a constant direction in time. The finite strain determinations for the two specimens have been done with pressure shadow fibres (following Durney & Ramsay 1973), and the standard deviation for the four calculated $1 + e_1$ values is indicated. It can be seen that in this representation greater variations in the determined finite strain values are not important above $1 + e_1 > 4$, because of the asymptotic trend of the curves. The amount of rotational deformation recorded in the two specimens is below the value required for simple shear.

The alternative model explains the obliquity between macroscopic cleavage and crystallographic and grain-shape fabric with a later deformation event, which has overprinted completely the microfabric related to the macroscopic cleavage and has led to the formation of a second cleavage. The observed obliquity, as well as the grain shapes, record the finite strain of this event, and the *c*-axis maximum is parallel to the compression direction as inferred from the microstructures of this second-phase deformation. This interpretation is supported by the result of experimental deformation of calcite in simple shear of Friedman & Higgs (1981).

Figure 9 shows the shear directions of this late event projected onto the cleavage planes, assuming that the shear movement is parallel to the intersection of the plane defined by the *c*-axis maximum and the normal to the macroscopic cleavage, and the macroscopic cleavage plane itself. The amount of plunge of these directions probably does not reflect the original dips of the shear planes, because the inclination of the cleavage planes is partly due to recent vertical movements. Around the arc of the chain there exists a systematic change in shear direction (Fig. 9a). For sectors of the chain with a constant strike the directions from the same tectonic units define a point maximum (Fig. 9b). These data can be integrated into the overall deformation history of the Helvetic chain. We envisage the nappes being individualized, dislocated and deformed in a zone of overthrust shear between the overriding Pennine chain and those Helvetic sediments of the foreland which have not

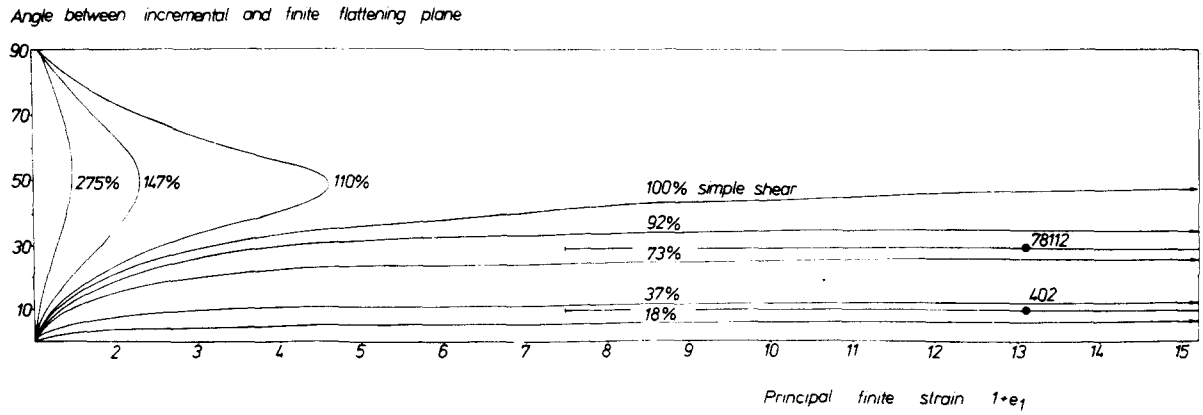

Fig. 8. Curves for the development of finite strain, assuming a steady state rotational deformation, modified after Pfiffner & Ramsay (1982), and applied for two Helvetic specimens. Increments of distortion ($e_1 = 0.1$) and incremental rotations (ω_i varied from zero through 5.455° or 100% simple shear to 20° or 275% simple shear) are superimposed.

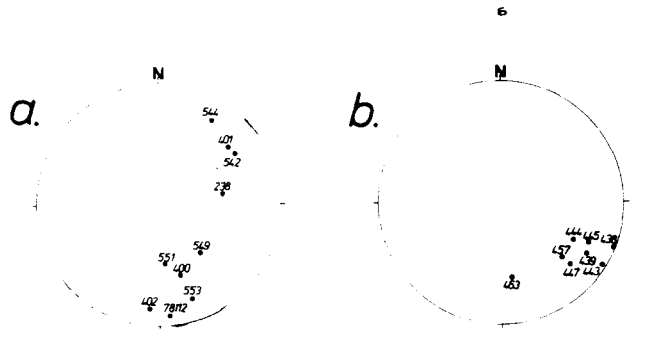

Fig. 9. Shear directions inferred from the microfabric of the Helvetic limestones. Plotted are the intersections of the macroscopic cleavage planes with the planes defined by *c*-axes and normals to the cleavage. Lower-hemisphere equal-area projection. Specimen localities are given in Fig. 4. (a) Shear directions west of Wildstrubel depression. (b) Shear directions east of Wildstrubel depression.

yet been reached by the Alpine tectonic movements. Within this zone, deformation becomes further localised in shear zones which separate the individual nappes (Casey & Huggenberger in press). The localisation of the shear zones follows the top-downwards rule, analogous to the proposed overthrust sequence from the top to the bottom of the nappe pile. The principal deformation features of the Helvetic rocks can be related to the formation of the individual nappes. The $1 + e_1$ finite strain trajectories (Fig. 1) show a distinctive pattern in each nappe. The variations of the principal extension directions could be related to a change of the overthrust shear direction during the deformation history. If the $1 + e_1$ finite strain trajectories are compared with the shear directions constructed from textural and microstructural data, the following conclusions emerge. East of the Wildstrubel depression the data given in Fig. 9 (b) define a SW–NE shear direction for the Doldenhorn nappe, the tectonic equivalent of the normal limb of the Morcles nappe (localities are indicated in Fig. 1). This direction does not correspond with the $1 + e_1$ finite strain trajectories of the normal limb of the Morcles–Doldenhorn nappe, but with the finite extension direction of the inverted limb of the Morcles nappe. This suggests that calcite microstructure and texture in the normal limb developed contemporaneously with the main overthrust shear deformation in the inverted limb. The amount of deformation recorded in the grain-shape fabric of the second cleavage is an order of magnitude smaller than the amount of deformation recorded by the finite strain markers. West of the Wildstrubel depression there are less crystallographic and microstructural data from which to determine a statistical shear direction for the individual units; a general trend is however visible in the data given in Fig. 9 (a). Three directions from specimens of the normal limb of the Morcles nappe, 402, 78112 and 549, are within the data spread of Fig. 9 (b). Westwards, around the arc of the chain, there is a change of direction towards SW–NE (specimen 544). The inverted limb data also show a noncoincidence with the $1 + e_1$ finite strain trajectories (specimen 238 in Fig. 9a). The constructed shear directions are always in a more anticlockwise direction than the finite strain trajectories, as were the normal limb constructed shear directions in relation to the normal limb finite strain trajectories. Around the arc there is a change in the constructed shear directions from E–W (specimen 238) or SE–NW (specimens 549, 551 and 553) to NE–SW (specimens 542, 544). This overall rotation in the western part must be related to late dextral shear movements in the root zone, for which independent evidence exists (Ayrton 1980).

The last deformation episode, which is recorded in the Helvetic rocks, is *e*-twinning, with, in the case of specimen 447 (Fig. 6) a compression direction parallel to the macroscopic cleavage.

Acknowledgements—Martin Casey and Stefan Schmid introduced us to texture goniometry. The pole figures were rotated using a program by Martin Casey. We thank Martin Casey, John Ramsay and Stefan Schmid for helpful and stimulating discussions. Comments on the manuscript by M. Casey, A. Pfiffner, J. G. Ramsay, J. Ridley and S. M. Schmid are gratefully acknowledged.

D.D. was supported by Schweizerischer Nationalfonds, Project No. 5.521.330.880/5.

REFERENCES

Ayrton, S. 1980. La géologie de la zone Martigny-Chamonix (versant suisse) et l'origine de la nappe de Morcles (un exemple de subduction continentale). *Eclog. geol. Helv.* **73**, 137–172.

Badoux, H. 1963. Les bélemnites tronçonnées de Leytron (Valais). *Bull. Soc. Vaudoise des Sciences Naturelles* **68**, 233–239.

Badoux, H. 1965. Déformation du Lias inférieur de la nappe du Wildhorn à Drône (Valais). *Eclog. geol. Helv.* **58**, 999–1001.

Badoux, H. 1970. Les oolites déformées du Vélar (massif de Morcles). *Eclog. geol. Helv.* **63**, 539–548.

Casey, M. & Huggenberger, P. in press. Numerical modelling of finite-amplitude similar folds developing under general deformation histories. *J. Struct. Geol.*

Casey, M., Dietrich, D. & Ramsay, J. G. 1983. Methods for determining deformation history for chocolate tablet boudinage with fibrous crystals. *Tectonophysics* **92**, 211–239.

Casey, M., Rutter, E. H., Schmid, S. M., Siddans, A. W. B. & Whalley, J. S. 1978. Texture development in experimentally deformed calcite rocks. *Proc. 5th Int. Conf. Textures of Materials*, Springer, Berlin, 231–240.

Chapple, W. M. 1968. Finite homogeneous strain and related topics. In *Rock Mechanics Seminar* (edited by Riecker, R. E.). *Spec. Rep. Terrestrial Sci. Lab.* Air Force Cambridge Research Laboratory, Bedford, Mass.

Collet, L. W. 1927. *The Structure of the Alps.* Arnold, London.

Dietrich, D. & Song, H. 1982. The fabric of calcite tectonites from the Helvetic root zone. *Mitt. geol. Inst. ETH Univ. Zürich* **239a**, 78–80.

Dietrich, D., Song, H. & Casey, M. 1981. An attempt at a kinematic interpretation of the root zone of the Helvetic nappes, Western Switzerland. *J. Struct. Geol.* **3**, 185–195.

Dietrich, D., McKenzie, J. A. & Song, H. 1983. Origin of calcite in syntectonic veins as determined from carbon-isotope ratios. *Geology* **11**, 547–551.

Durney, D. W. 1971. Deformation history of the Western Helvetic nappes, Valais, Switzerland. Ph.D. thesis, University of London.

Durney, D. W. & Ramsay, J. G. 1973. Incremental strains measured by syntectonic crystal growth. In: *Gravity and Tectonics* (edited by DeJong, K. & Scholten, R.). Wiley, New York, 67–96.

Friedman, M. & Higgs, N. G. 1981. Calcite fabrics in experimental shear zones. In: *Mechanical Behaviour of Crustal Rocks. Geophysical Monograph* **24**, 11–27.

Gray, D. R. & Durney, D. W. 1979. Investigations on the mechanical significance of crenulation cleavage. *Tectonophysics* **58**, 35–79.

Handin, J. W. & Griggs, D. 1951. Deformation of Yule marble—Part II. Predicted fabric changes. *Bull. geol. Soc. Am.* **62**, 863–886.
Heim, A. 1921. *Geologie der Schweiz*. II/1. Tauchnitz, Leipzig.
Kern, H. 1977. Preferred orientation of experimentally deformed limestone marble, quartzite and rock salt at different temperatures and states of stress. *Tectonophysics* **39**, 103–130.
Kern, H. & Wenk, H. R. 1982. Calcite-texture development in experimentally induced ductile shear zones. *Mitt. geol. Inst. ETH Univ. Zürich* **239a**, 154–156.
Kvale, A. 1966. *Gefügestudien im Gotthardmassiv und den angrenzenden Gebieten*. Sonderveröffentlichung Schweiz. Geotech. und Schweiz. Geol. Kommission, Kümmerly & Frey, Bern.
Pfiffner, O. A. & Ramsay, J. G. 1982. Constraints on geological strain rates: arguments from finite strain states of naturally deformed rocks. *J. geophs. Res.* **87**, 311–321.
Ramsay, J. G. 1967. *Folding and Fracturing of Rocks*. McGraw-Hill, New York.
Ramsay, J. G. 1980. Shear zone geometry: a review. *J. Struct. Geol.* **2**, 83–99.
Ramsay, J. G. 1981. Tectonics of the Helvetic nappes. In: *Thrust and Nappe Tectonics* (edited by McClay, K. & Price, N. J.). *Spec. Publs geol. Soc. Lond.* **9**, 293–309.
Ramsay, J. G. 1982. Variations in linear and planar fabrics in the western Helvetic nappes, Switzerland. *Mitt. geol. Inst. ETH Univ. Zürich* **239a**, 230–232.
Ramsay, J. G., Casey, M. & Kligfield, R. 1983. Shear zones and nappe tectonics in the Helvetic fold/thrust belt. *Geology* **11**, 439–442.
Rutter, E. H. & Rusbridge, M. 1977. The effect of non-coaxial strain paths on the crystallographic preferred orientation development in the experimental deformation of a marble. *Tectonophysics* **39**, 73–86.
Schmid, S. M. 1982. Laboratory experiments on rheology and deformation mechanisms in calcite rocks and their application to studies in the field. *Mitt. Geol. Inst. ETH Univ. Zürich* **241**, 1–62.
Schmid, S. M., Casey, M. & Starkey, J. 1981. The microfabric of calcite tectonites from the Helvetic nappes (Swiss Alps). In: *Thrust and Nappe Tectonics* (edited by McClay, K. & Price, N. J.). *Spec. Publs. geol. Soc. Lond.* **9**, 151–158.
Siddans, A. W. B. 1976. Deformed rocks and their textures. *Phil. Trans. R. Soc.* **A283**, 43–54.
Trümpy, R. 1980. *Geology of Switzerland. Part B: Geological Excursions. Excursion I. Helvetic Alps of Western Switzerland*. Masson, H., Herb, R. & Steck, A. Wepf & Co., Basel, 109–153.
Turner, F. J. 1953. Nature and dynamic interpretation of deformation lamellae in calcite of three marbles. *Am. J. Sci.* **251**, 276–298.
Turner, F. J. & Ch'ih, C. S. 1951. Deformation of Yule marble—Part III. Observed fabric changes due to deformation at 10,000 atmospheres confining pressure, room temperature, dry. *Bull. geol. Soc. Am.* **62**, 887–906.
Turner, F. J., Griggs, D. T., Clark, R. H. & Dixon, R. H. 1956. Deformation of Yule marble—Part VII. Development of oriented fabrics at 300–500°. *Bull. geol. Soc. Am.* **67**, 1259–1294.
Turner, F. J. & Weiss, L. E. 1963. *Structural Analysis of Metamorphic Tectonites*. McGraw-Hill, New York.
Wenk, H. R. Venkitsubramanyan, C. S. & Baker, D. 1973. Preferred orientation in experimentally deformed limestone. *Contr. Miner. Petrol.* **38**, 81–114.

APPENDIX

A graphic method for the determination of the compressive stress direction from e-twinning in calcite

This method is based on the geometry of mechanical twinning on $[01\bar{1}2]$ as established by Handin & Griggs (1951). The development of the individual twin sets allows progressive elimination of regions in which the compressive stress direction can not be located.

The angle between the *c*-axis of a calcite host crystal and the poles to the *e*-twin planes is 26°. The direction of *e*-twin gliding is given by the edge [*e*:*r*], and the sense is towards the *c*-axis of the host. The procedure is as follows.

(1) Plot the measured *c*-axis, c, the *e*-plane and its pole, e_1, on an equal-area net.
(2) Find [*e*:*r*], the direction of twin gliding, constructing a great circle through e_1 and c; the intersection of the great circle with the *e*-plane is $[e_1{:}r_2]$ (Fig. 10a).
(3) Divide the net into quadrants for compressive and extensional (or least compressive) stresses according to the known direction and sense of twin gliding (Fig. 10a); the quadrant containing c is the extension quadrant.

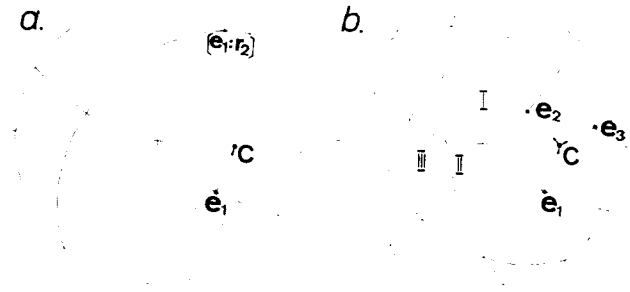

Fig. 10 (a) Compression and extension quadrants of possible stresses for *e*-twinning. Equal-area projection. e_1 is the pole to the e_1 twin plane, $[e_1{:}r_2]$ is the direction of twin gliding on e_1, the dotted areas are the compression quadrants for twin gliding on e_1. (b) Compression and extension quadrants of possible stresses for three sets of *e*-twins in a crystal. The dotted areas are compression quadrants. If the compressive stress is located in area I, only one set of twins on the e_2 plane is possible. If the compressive stress is located in area II, twinning on e_1 and e_2 is possible. If the compressive stress is located in the empty area, *e*-twinning is not possible.

(4) It is evident from Fig. 10 (a), that there is a minimum angle between any possible direction of compressive stress and the *c*-axis. This angle is greater in the case of the simultaneous development of two or three twin sets in a crystal, as shown in Fig. 10 (b) and below.
I *e*-twin set in a crystal: $\sigma_1 \wedge c > 26°$.
II *e*-twin sets in a crystal: $\sigma_1 \wedge c > 44.5°$, $\sigma_1 \wedge e > 38°$.
III *e*-twin sets in a crystal: $\sigma_1 \wedge c > 64°$.
This means in the case of the development of one twin set, that there is a small-circle domain with a radius of 26° around the axis of the compressive stress which should not contain *c*-axes. Furthermore, the movement direction is away from the stress axis and towards the *c*-axis. The radius of the small circle would be 44.5° in the case of two *e*-twins, and 64° in the case of three *e*-twins.
(5) Plot *c*-axes and poles to *e*-planes from calcite crystals with one, two or three twin sets separately, and indicate the direction of twin gliding. Find the compressive stress direction as the centre of the manually constructed small circles. Examples are given in Figs. 6 (a) & (b) and 11 (a) & (b).

Turner (1953) proposed a different method for stress determination from twinning. His method is based on the theoretical consideration, that "The unique compressive stress C that would most effectively initiate twin gliding on e_1 of a given grain is directed in the zone of e_1 and [0001] at 45° to e_1 and at 71° to [0001]" (Turner & Weiss 1963, p. 242, also Handin & Griggs 1951). The results of this method are given, for comparison, in Fig. 11 (c). The overall data spread by Turner's method can be great, as particularly evident for specimen 490 (Fig. 11c) because the most effective stress direction can differ significantly from the real stress axis responsible for twinning in a grain. The determination of a maximum which indicates σ_1 can therefore be inaccurate.

Kvale (1966, p. 54) used a method which is similar to our method but, as a result of limiting his analysis to two dimensions instead of three, he obtained different minimum values for the angle $\sigma_1 \wedge c$.

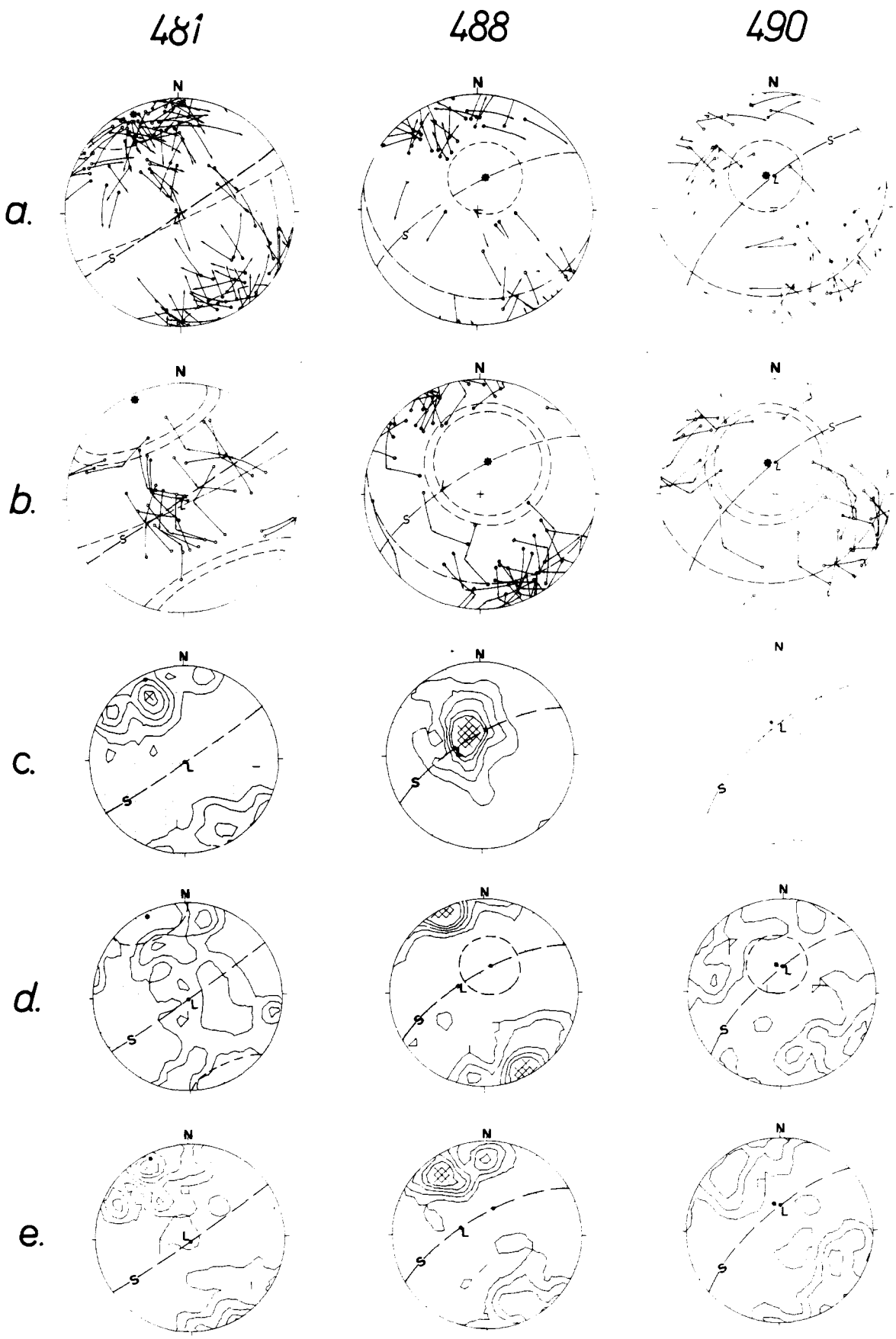

Fig. 11. Specimens 481 from Andermatt and 488 and 490 from the Furka Pass. Results of U-stage measurements. Lower-hemisphere equal-area projection. Asterisk indicates the orientation of σ_1 for *e*-twinning; for the method of stress determination see Appendix. *S*, Plane of macroscopic cleavage; *L*, macroscopic lineation (a) Pole figures for *e* and *c* of calcite grains with one *e*-twin set developed. White circles, poles to *e*-twin planes. Arrows show the movement direction for *e*-twinning from *e*-poles to *c*-axes. (b) Pole figures for *e* and *c* of calcite grains with two or three *e*-twin sets developed. (c) Pole figures for σ_1 for *e*-twinning determined by Turner's method. 481, 134 data, contours at 1, 2, 3, 4, 5 points per 0.7% area; 488, 68 data, contours at 1, 2, 3, 4, 5 points per 1.5% area; 490, 75 data, contours at 1, 2, 3, 4, points per 1.3% area. (d) Pole figures for calcite *c*-axes from host grains. 481, 123 data, contours at 1, 2, 3 points per 0.8% area; 488, 69 data, contours at 1, 2, 3, 4, 5 points per 1.4% area; 490, 68 data, contours at 1, 2, 3 points per 1.5% area. (e) Pole figures for calcite *e*-twin planes. 481, 147 data, contours at 1, 2, 3, 4, 5 points per 0.7% area; 488, 96 data, contours at 1, 2, 3, 4, 5 points per 1% area; 490, 91 data, contours at 1, 2, 3, 4, 5 points per 1.1% area.